ASSOCIAZIONE ITALIANA per l'INGEGNERIA del TRAFFICO e dei TRASPORTI AIIT

Giordano Editore

# Developing a framework for using Structure-from-Motion techniques for Road Distress applications

**Ronald Roberts[1*], Laura Inzerillo[1] , Gaetano Di Mino[1]**

[1]*University of Palermo, Viale delle Scienze ed.8, 90128, Palermo, Italy*

**Abstract**

On Urban road networks, road agencies need to quickly identify road pavement distresses in order to identify appropriate maintenance and rehabilitation strategies. This is integral as agencies are plagued with financial and time constraint issues. There have been several attempts over the last few years to identify new solutions and techniques to solve these issues. Several of these have shown merit and accuracy in identifying distresses. However, the techniques in many instances are not correlated to available distress identification standards. One of the considered techniques is the use of Structure-from-Motion, which tries to recreate 3D distress models for identification and analysis. This paper considers this methodology and attempts to integrate it with measurement requirements used by distress manuals to illustrate how the technique can be used with real-world industry standards and practices. Case studies of different measurement types, on an urban road in Palermo, Italy, are considered. The results from these examples show that the technique replicates pavement distresses of varying measurement requirements and the paper presents a workflow of how it can be utilized to help optimize the pavement management system and their connections to different distress identification manuals worldwide.

*Keywords:* Structure-from-Motion; 3D Modelling; Pavement Distresses; Pavement Management System

## 1. Introduction

Road agencies worldwide are faced with difficult decisions for road maintenance and rehabilitation strategies. There are significant financial challenges evidenced by the [illegible] Federation (IRF), 2018). Also challenging is the fact that in most instances these strategies are based on manual road conditional surveys (Radopoulou and Brilakis, 2016) which can be subjective and time-consuming. Therefore, it has become a necessity to find solutions which can help automate this process and reduce costs associated with these surveys. This will help to better optimize the strategies and this is important as it has been clearly shown that maintenance carried out earlier in the pavement's life cycle is cheaper, can produce significant savings (Bazlamit et al., 2017) and help to elongate the pavement's life cycle.



* Corresponding author: Ronald Roberts (ronaldanthony.roberts@unipa.it)

To ensure this optimization is done, the use of a Pavement Management System (PMS) has been seen as a common approach as it aims to assign available funds to the most valued construction, maintenance and rehabilitation strategies (Peterson, 1987).

Within the PMS, pavement distress information is collected and utilized by agencies to get an overall road system rating using standardized performance indices. There are several of these. One such rating is the Present Serviceability Rating (PSR), developed by the American Association of State Highway Officials (AASHO) (Carey Jr and Irick, 1960). The PSR is a subjective rating, based on experiences and judgement of road users. The PSR was used to develop the Present Serviceability Index (PSI) which is based on road characteristics of pavement roughness and the distresses of patching, rutting and cracking. Utilizing pavement smoothness and ride-ability, the International Roughness Index (IRI) was developed, but this index typically requires specialized equipment to measure features utilizing built-in algorithms (Paterson, 1986). Using the subjective ratings of distresses, the U.S. Army Corps of Engineers (USACE) developed the Pavement Condition Index (PCI) (American Society for Testing and Materials. (ASTM), 2018). The PCI is widely used and respected and is based on calculating deduct values allocated to each distress type based on the area affected and severity level. Subsequently these values are subtracted from the total to obtain a rating of 0 – 100 (where 0 = a failed pavement) which is related to a pavement condition rating ranging from 'Good' to 'Failed'. The PCI has been used as a parameter for the evaluation of urban road networks (Shah et al., 2013). Recent work on this was done with respect to the Urban Italian Road Network, wherein the PCI has been considered as a good basis for finding a new distress identification system for the Italian Urban network (Loprencipe and Pantuso, 2017).

### *1.1 Distress Identification Manuals*

For these indices to be applied in the PMS, agencies rely on distress identification manuals to standardize the subjective nature of the surveys. There are several distress manuals worldwide, which aim to describe the distresses and give descriptions on how to identify them and to measure their severity. For this study, six of these were analyzed covering North America, Europe and Australia. These are; Manual 1: (American Society for Testing and Materials. (ASTM), 2018), Manual 2: (Miller and Bellinger, 2014), Manual 3: (British Columbia Ministry of Transportation and Infrastructure Construction Maintenance Branch 2016), 2016) Manual 4: (Bertrand et al., 1998), Manual 5: (Direzione Generale Infrastrutture e Mobilità Milano, 2005) and Manual 6: (VicRoads, 2009). Some of the manuals have the severity being defined by specific dimensions of the distress and then have the distress itself recorded as a ratio of the distressed area to the total area (e.g. ASTM) whilst others define the severity directly by this ratio. Generally, distresses can be broken down into five categories based on the cause of the distress: surface texture deficiencies, deterioration, deformation, patching and structural distress (Di Mino et al., 2014) and typically, they are measured in one of three ways as shown in Table 1. Using these definitions, the study focused on showing how the methodology can yield the requisite quantitative data for each of these categories.

Table 1: Breakdown of distresses by measurement type

| *Units of measurement used by manuals* | *Distresses typically covered* |
|---|---|
| Linear meters | Longitudinal and Transverse cracking, Edge cracking, Joint reflection, Lane/shoulder drop off |
| Number of occurrences | Potholes |
| Square meters | Alligator cracking, Bleeding, Block cracking, Corrugation, Depression, Patching and Utility cut patching, polished aggregate, railroad crossings, rutting, shoving, slippage cracking, swelling, ravelling, weathering |

Given these groups, an analysis of how these types of distresses are defined by the manuals could be carried out. For the purpose of this study, an example of each type was done as this is shown in Table 2. The types chosen were Longitudinal/Transverse cracking, Potholes and Rutting. The reason for this is related to both the location of the case study (Italy) and the importance of the distresses. Cracking was chosen as it represents the largest number of pavement distress on Urban roadways in Italy (Loprencipe and Pantuso, 2017). Rutting was chosen given its importance to the design of the pavement itself and given the fact that when a pavement begins to suffer this type of distress its pavement life is in its final stages and finally potholes were chosen as this distress represents the only one typically measured based on a 'number of occurrences' method. A comparison of the severity definition in the manuals is given below.

Table 2: Examples of definitions of distress severity given by distress manuals

| Manual | Longitudinal Cracking | | | Pothole | | | Rutting | | |
|---|---|---|---|---|---|---|---|---|---|
| | Low | Medium | High | Low | Medium | High | Low | Medium | High |
| 1 | width< 10mm | 10mm≥ width≥ 75mm | width ≥76mm | depth: 13 to ≤25mm and ø <450mm or depth: 25 to ≤50mm and ø <200mm | depth 13 to ≤25mm and 450mm>ø>75 0mm **or** depth >25mm to ≤50mm and 200mm<ø<45 0mm **or** depth:>50mm and 200mm<ø<45 0mm | depth > 25mm and ≤50mm and 450mm< ø <750mm or depth:> 50mm and 450mm< ø<750mm | depth of 6 to 13 mm | depth >13 to 25 mm | depth >25 mm |
| 2 | Mean width ≤ 6 mm | Mean width > 6 mm and ≤ 19 mm or any crack with mean width ≤ 19 mm | Mean width > 19 mm or any crack with mean width ≤ 19 mm | < 25 mm deep. | 25 to 50 mm deep. | > 50 mm deep. | Des. | Des. | Des. |
| 3 | mean unsealed crack width < 5mm | mean unsealed crack width 5-20mm | mean unsealed crack width >20mm | area > 175 cm² (~150mm ø) and < 25mm deep | area > 175 cm² (~150mm ø) and 25 to 50mm deep | area > 175 cm² (~150mm ø) and > 50mm deep | depth < 10 mm | depth of 10 to 20 mm | depth > 20 mm |
| 4 | Des. | Des. | Des. | ø < 150mm | ø > 150mm | | noticeable depth of 5 to 15 mm | significant depth of 15 to 30 mm | deep rut depth > 30 mm |
| 5 | Width <2mm | 2mm> Width <10mm | width> 10mm | ø<100mm and depth <50mm | 100<ø<300mm and depth <25mm | ø>300mm and depth >25mm | depth<15 mm | depth>15 to <30mm | depth> 30mm |
| 6 | affecting < 10% of area. | affecting 10 – 20% of area. | affecting > 20% of area | Measured in terms of the area affected but grouped under current required 'maintenance patching' | | | affecting < 10% of area | affecting 10 – 30% of area | affecting > 30% of area |

Note: ø = Diameter, Des. = Descriptive definition, Manual numbers are as earlier defined in section 1.1.

As seen in Table 2, there are varying numerical definitions of the distress types and measurement methods. There is thus no uniformity amongst the definitions and some of these deviations are quite large. For instance, with the definition of longitudinal cracking between manuals: the high severity is defined as a crack with a width over 19mm for Manual 2 while for Manual 1 it is defined as one with a width over 76mm. These parameters are however based on the location of the assessment as it further stresses that any definition system should be based on local conditions rather than the arbitrary use of a distress identification manual.

Nevertheless, the important takeaways from Tables 1 and 2 are the measurement requirements for practitioners faced with the task of a conditional survey regardless of the locations. Using these analyses, the requirements can be grouped as shown in Fig. 1. This is important, as any method for carrying out the surveys must meet these criteria to adequately provide information towards defining the overall road condition parameters such as the PCI for the PMS.

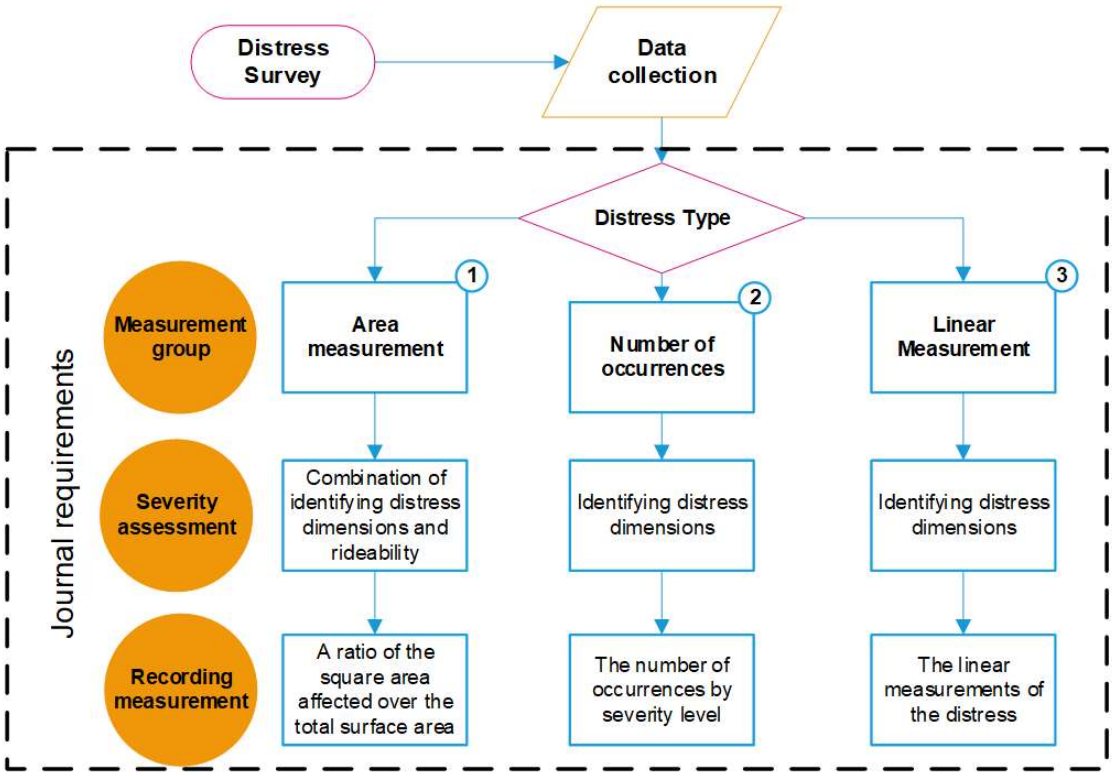


Figure 1: Requirements to identify and analyze pavement distressed as defined by manuals.

### *1.2 The use of 3D Image-based Modelling of Pavement Distresses*

Given the importance of identifying the distress and their severities, there have been several attempts over the years to find new methodologies for distresses identification (Coenen and Golroo, 2017) to satisfy the requirements shown in Fig.1. The use of 3D modelling has been used, but its use has relied on expensive and advanced equipment to produce information (Petitclerc et al., 2018). A cheaper alternative is the use of Stereovision approaches including photogrammetry and Structure-from-Motion (SfM).

These approaches are not new (Wang, 2011) (Ahmed et al., 2011) but recent research in other fields such as architecture and archaeology have shown improved accuracies in software packages and algorithms (F. Remondino et al., 2017) with studies successfully using these for pavement distress application establishing the accuracy of the methodology by comparing results to laser scanners (Inzerillo et al., 2018).

SfM is the process by which metric information is obtained about an object by utilizing overlapping 2D imagery (Westoby et al., 2012). In the process, images are captured circling the object at different angles with an overlap of 70-90% and then using algorithms in a now-standard and simple workflow which can be followed easily by anyone. Within the SfM software, images are aligned and the object's position in space is established to reconstruct a 3D model (Verhoeven, 2011). An example of a dataset captured over a distressed pavement is shown in Fig.2. The generated 3D models can be used to generate metric information about the distress and therefore its severity. Given these studies, this study aims to match the requirements of the pavement distress manuals to the workflows of SfM to validate whether the methodology can be used for different distress types and whether it can produce the information required to yield the performance indices and in turn the input data for the PMS at cheaper costs.

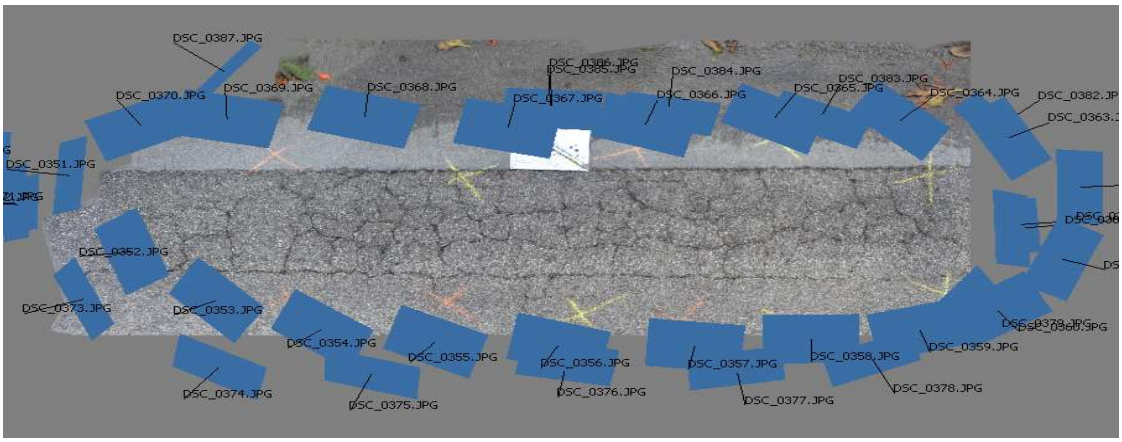


Figure 2: Example of Dataset of a pavement

## 2. Methodology

### *2.1 SfM technique and workflow*

Based on the distress measurement groupings as shown in Table 1, a case study was conducted in Palermo, Italy on a distressed urban pavement highlighting three specific distresses: 1. longitudinal cracking, 2. pothole and 3. rutting. The study developed 3D models of each distress using the SfM workflow and setup, which is illustrated in Fig.3. The illustrated workflow and model construction was carried out in Agisoft PhotoScan and the 3D model geometric analysis was done in Rhinoceros 5®. Within Fig. 3, the manual requirements for each of the three distress are also shown for reference to each measurement type.

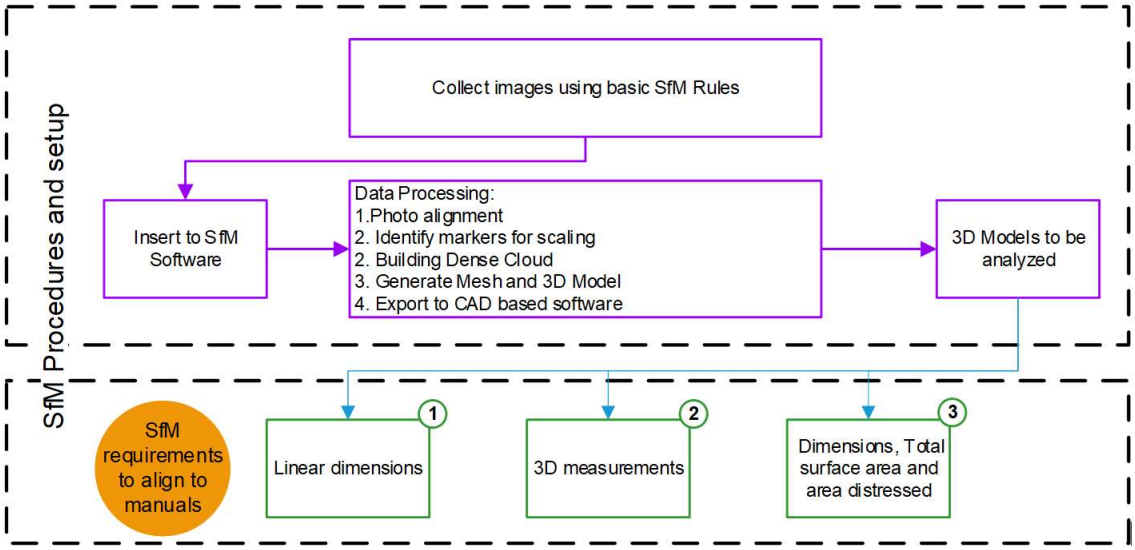


Figure 3: SfM workflow utilized for Conditional Pavement Surveys.

### *2.2 Experimental setup*

The resulting models from the SfM process are normally interpreted with respect to the Ground sampling distance (GSD), which represents the measured distance between two consecutive pixel centres as measured on the ground. The lower this value is, the higher is the spatial resolution. The GSD represents the smallest details that can be observed on an image. (Remondino et al., 2017). This is critical, as this will define the resolution of the resulting 3D models and the level of detail possible from replicated models. Based on the manual measurement requirements, as shown in Table 2, the smallest change needed is 1mm. Within a 3D model the smallest details visible and measurable are two to three times the value of the GSD (Höhle, 2013)) and therefore the GSD should be two to three times smaller than the required detail measurement. As the smallest detail required for the survey is 1mm, the GSD, therefore, needs to be no greater than 0.33mm. A smaller GSD would, of course, produce a higher spatial resolution and clearer model. The GSD is related to several parameters including the focal length of the camera, the distance from the object at which the images are taken, and the real size of one pixel on the image as depicted in Equation 1.

$$D = \frac{GSD \times f}{px_{size}} \tag{1}$$

Where D= Object Distance, GSD= ground sampling distance, $f$= focal length and $px_{size}$= pixel size (as defined by the ratio of the camera's sensor height to the image height). For this instance and for SfM surveys for pavement distresses, we can affix the GSD as 0.33mm; therefore, the equation can be rewritten as shown in Equation 2:

$$D = \frac{0.33 \times f}{px_{size}} \tag{2}$$

These parameters can be manipulated to produce the required GSD. Whilst the focal length and pixel size can be fixed for a survey, the object distance can vary slightly as the surveyor moves around the object. Therefore, the actual object distance aimed for should be less than the calculated one to cater for deviations. The parameters of focal length depend on the camera used and these have to be determined before the survey to ensure the resulting model can provide adequate 3D resolutions to allow for severity measurements. Different cameras and even smartphones can be used for this once this calculation is done but with reducing camera quality (e.g. the camera's focal length), the object distance will need to be decreased. However, given the high camera resolutions now available on smartphones this will not be a problem moving forward. Using this setup, the surveys were carried out using a Nikon D5200 camera with a resolution of 6000 x 4000 pixels. Each survey took approximately 10 minutes and the survey parameters are shown in Table 3 below. Printed coded markers from the commercial software were also used to scale the models and establish the necessary accuracy to determine 1mm estimations with an error of less than 0.1mm.

Table 3. Parameters used for the survey

| Survey parameter | Longitudinal crack | Pothole | Rut |
|---|---|---|---|
| Distance from pavement (m) | 1.73 | 1.21 | 2.17 |
| Number of photos taken | 19 | 57 | 28 |

### *2.3 3D Model setup and analysis*

After the image survey, the 3D models were created within the SfM software as described in Fig. 3. Measurements were then obtained by importing models into the modelling software Rhinoceros 5® to use Computer Aided Drafting (CAD) tools for geometrical analysis. The models were scaled and rotated to align them in an absolute reference system with units set in mm. After this, a review of the models was done to ensure there were no errors in the topology. Sections can then be made in both horizontal and vertical planes to extract curvilinear profiles and sections. Using the software, multiple parallel longitudinal sections are created to define distress profiles. Each created profile can be isolated and analyzed. This, therefore, leads to the identification of the required geometrical features of maximum depths and widths and area distressed. For each derived model, the geometrical analysis was based on what was required by the manuals i.e. length of the crack, depth of rutting and area distressed, depth and diameter of the pothole.

## 3. Results and Discussions

### *3.1 Models developed*

The models' physical characteristics are given in Table 4, where the achieved GSD is showcased which meets the previously mentioned criteria thus allowing an assessment of the distress' physical dimensions. Using the CAD software, the geometrical analysis was done to evaluate the distresses. This analysis, therefore, allowed a severity determination. A few sections of each distress are shown in Fig. 4. These represent only a glimpse of the

possible sectional analyses. Shown in the figure are the longitudinal crack's width at various points along its body, the pothole's diameter and depth and the rutted area along with its depth. These measurements satisfy the requirements of the manuals and based on the analysis the severities can be identified as follows: Longitudinal crack (Low severity), Pothole (High severity) and rutting (High severity), according to ASTM, 2018 (Manual 1). This is an example of one manual but regardless of the manual, the method can yield the required measurement. With the models, one can also obtain additional measurements such as depth of the crack, actual volume of the pothole and volume of the rutted area.

Table 4. Result characteristics of replicated SfM models

| Model parameter | Longitudinal crack | Pothole | Rut |
|---|---|---|---|
| Mesh faces created in SfM software | 2,258,886 | 4,814,789 | 12,590,502 |
| GSD aimed for (mm/pixel) | 0.33 | 0.33 | 0.33 |
| Actual GSD achieved (mm/pixel) | 0.183 | 0.151 | 0.175 |

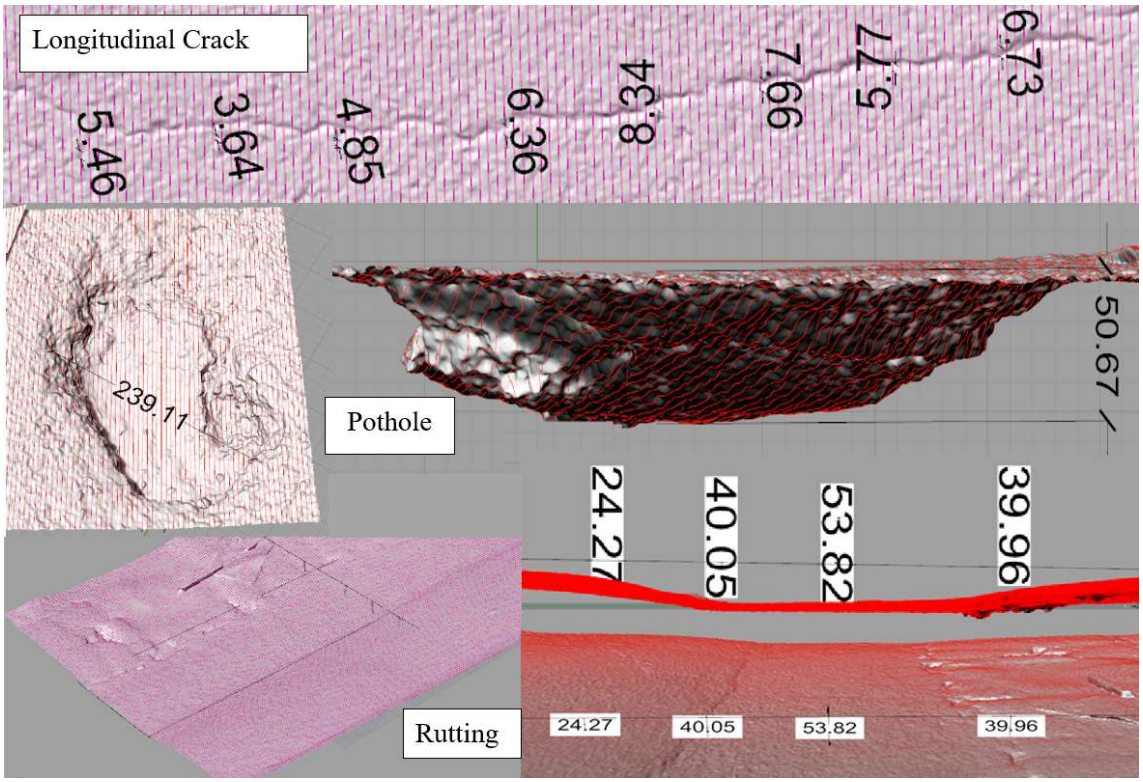


Figure 4: Example cross-sections of created 3D Models showing aspects of geometrical analysis (dimensions in mm)

### *3.2 Developed workflows*

Given the replicated models, the methodology adequately obtains the required dimensions and therefore a workflow can be drawn for each. Also of interest are the additional measurements which can be obtained which provide further information for distress analysis and can be used to generate greater assessments of damages. These additional details are not possible through visual inspections and can be used to further

bolster the PMS input data and create a new metric for assessment in the future. The workflows developed are shown in Fig. 5.

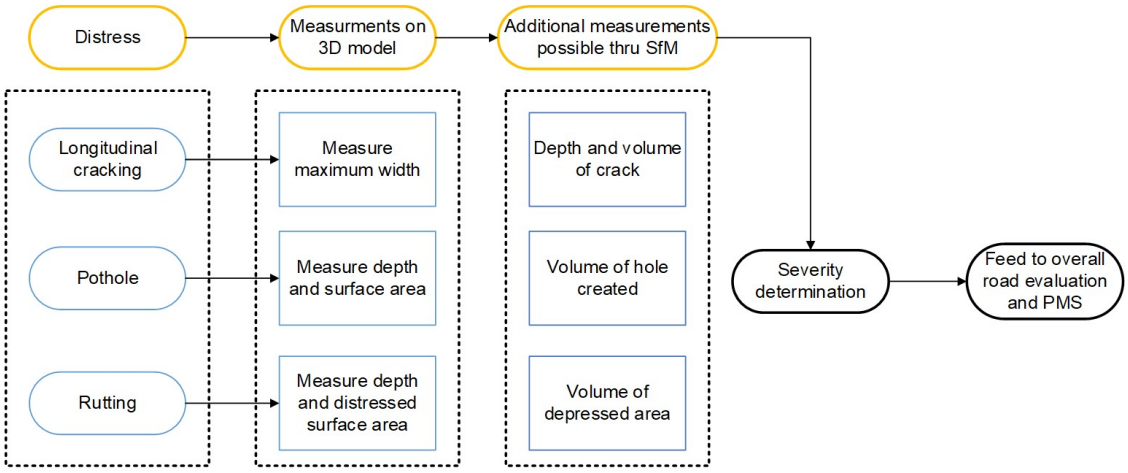


Figure 5: Workflow for utilizing SfM Image-based modelling.

## 4. Conclusions and recommendations

The study explored different pavement manuals and techniques used by road agencies worldwide to evaluate pavement conditions. It was shown that these contain several differences in the severity levels definitions in terms of numerical values and the specific metric requirement. However, there are certain commonalities such as the measurement method groupings, which can be used to guide new detection methods. Using these, workflows were established to show what these requirements are.

A case study was subsequently developed to demonstrate how 3D Image-based modeling can be used to both replicate pavement distresses and fulfil manual requirements to determine severities. Using three real world examples, from each associated category, the process was validated, establishing not only the necessary requirements of the manuals but also additional features and measurements along with cross-sectional analyses not possible with visual and manual surveys. Based on these results, a workflow of how the technique can be utilized for different measurement requirements was created which can help the optimization the data acquisition within the pavement management system.

Future work will focus on automation of these workflows and recognizing patterns within the models for identification along with the utilization of the additional distress measurement information for a more robust assessment of distresses and their severities.

*References*

Ahmed, M., Haas, C.T., Haas, R. (2011) "Toward low-cost 3D automatic pavement distress surveying: The Close Range Photogrammetry Approach", *Canadian Journal of Civil Engineering*, 38(12), pp. 1301–1313. https://doi.org/10.1139/L11-088.

American Society for Testing and Materials. (ASTM). (2018) *ASTM D 6433 -18 Standard Practice for Roads and Parking Lots Pavement Condition Index Surveys*, West Conshohocken. https://doi.org/10.1520/D6433-18.

Bazlamit, S.M., Ahmad, H.S., Al-Suleiman, T.I. (2017) "Pavement Maintenance Applications Using Geographic Information Systems", *Procedia Engineering*, 182, pp. 83-90. https://doi.org/10.1016/j.proeng.2017.03.123

Bertrand, L., Boutonnet, M., Cazeneuve, J., Chabrol, J., Dauzats, M., Griselin, J.., Coquereau, A., Poilane, J.., Robert, B., Lepert, P., Siffert, M. (1998) *Catalogue des degradations de surface des chaussees*. Paris.

British Columbia Ministry of Transportation and Infrastructure Construction Maintenance Branch (2016) *Pavement surface condition rating manual , Fifth edition 95,* British Colombia, Canada

Carey Jr, W.N., Irick, P.E. (1960) "*The pavement serviceability performance concept*", Highway Research Board Bulletin. 250, pp. 40–58.

Coenen, T.B.J., Golroo, A. (2017) "A review on automated pavement distress detection methods", *Cogent Engineering*, 4, pp. 1–23. https://doi.org/10.1080/23311916.2017.1374822

Di Mino, G., Salvo, G., Noto, S. (2014) "Pavement management system model using a LCCA - microsimulation integrated approach", *Advances in Transportation Studies*. 4, pp. 101-112. https://doi.org/10.4399/978885487354410

Direzione Generale Infrastrutture e Mobilità Milano. (2005). *Catalogo dei dissesti delle pavimentazioni stradali.* Milan, Italy.

Höhle, J. (2013) "Oblique Aerial Images and Their Use in Cultural Heritage Documentation" *ISPRS - International Archives of the Photogrammetry, Remote Sensing and Spatial Information Sciences*, XL-5/W2, pp. 349–354. https://doi.org/10.5194/isprsarchives-xl-5-w2-349-2013

International Road Federation (IRF) (2018) *IRF World Road Statistics 2018 (Data 2011 -2016)*. Brussels.

Inzerillo, L., Di Mino, G., Roberts, R. (2018) "Image-based 3D reconstruction using traditional and UAV datasets for analysis of road pavement distress", *Automation in Construction*, 96, pp.457-469. https://doi.org/10.1016/j.autcon.2018.10.010

Loprencipe, G., Pantuso, A. (2017) "A Specified Procedure for Distress Identification and Assessment for Urban Road Surfaces Based on PCI", Coatings 7(5), pp. 65. https://doi.org/10.3390/coatings7050065

Miller, J.S., Bellinger, W.Y. (2014) *Distress Identification Manual for the Long-Term Pavement Performance Program (Fifth Revised Edition)*. Virginia.

Paterson, W. (1986) "International roughness index: Relationship to other measures of roughness and riding quality", *Transportation Research Record: Journal of the Transportation Research Board*, 1084, pp. 49–59.

Peterson, D. (1987) *Pavement Management Practices. No. 135*. National Cooperative Highway Research Program Synthesis of Highway Practice, Washington, DC.

Petitclerc, B., Laurent, J., Sc, M., Habel, R., Sc, M. (2018) "Optimizing 3D Surface Characteristics Data Collection By Re-Using the Data for Project Level Road Design" *SURF 2018* - Proceedings from the 8th Symposium of Pavement Surface Characteristics - Vehicle to Road Connectivity, Brisbane, Queensland.

Radopoulou, S.C., Brilakis, I. (2016), "Improving Road Asset Condition Monitoring", *Transportation Resarch Procedia* 14, pp. 3004–3012. https://doi.org/10.1016/j.trpro.2016.05.436

Remondino, F., Nocerino, E., Toschi, I., Menna, F. (2017), "A critical review of automated photogrammetric processing of large datasets", *International Archives of the Photogrammetry, Remote Sensing and Spatial Information Sciences - ISPRS*

*Archives*, 42(W5), 591–599. https://doi.org/10.5194/isprs-archives-XLII-2-W5-591-2017

Shah, Y.U., Jain, S.S., Tiwari, D., Jain, M.K. (2013), "Development of Overall Pavement Condition Index for Urban Road Network", *Procedia - Social and Behavioral Sciences,* 104 ,pp. 332–341. https://doi.org/10.1016/j.sbspro.2013.11.126

Verhoeven, G. (2011), " Taking computer vision aloft -archaeological three-dimensional reconstructions from aerial photographs with photoscan", *Archaeological Prospection*. 18(1), pp. 67–73. https://doi.org/doi.org/10.1002/arp.399

VicRoads. (2009) *Guide to Surface Inspection Rating For Pavements Surfaced with Sprayed Seals and Asphalt*. VicRoads, Victoria.

Wang, K.C.P. (2011), "Elements of automated survey of pavements and a 3D methodology", *Journal of Modern Transportation*, 19, pp. 51–57. https://doi.org/10.1007/BF03325740

Westoby, M.J., Brasington, J., Glasser, N.F., Hambrey, M.J., Reynolds, J.M. (2012), ""“Structure-from-Motion” photogrammetry: A low-cost, effective tool for geoscience applications", Geomorphology. 179(2012), pp. 300-314. https://doi.org/10.1016/j.geomorph.2012.08.021

*Acknowledgements*

The research presented in this paper was carried out as part of the H2020-MSCA-ETN-2016. This project has received funding from the European Union’s H2020 Programme for research, technological development and demonstration under grant agreement number 721493.